HHS Public Access

Author manuscript

Hear Res. Author manuscript; available in PMC 2019 July 01.

Published in final edited form as:

Hear Res. 2018 July ; 364: 129–141. doi:10.1016/j.heares.2018.03.014.

Paraquat initially damages cochlear support cells leading to anoikis-like hair cell death

Jianhui Zhang[1,2], **Hong Sun**[1,2], **Richard Salvi**[1,2,3], and **Dalian Ding**[1,2]

[1]Department of Otorhinolaryngology Head and Neck Surgery, Xiangya Hospital, Central South University, China

[2]Center for Hearing and Deafness, University at Buffalo, Buffalo, NY, 14214, USA

[3]Department of Audiology and Speech-Language Pathology, Asia University, Taichung, Taiwan

Abstract

Paraquat (PQ), one of the most widely used herbicides, is extremely dangerous because it generates the highly toxic superoxide radical. When paraquat was applied to cochlear organotypic cultures, it not only damaged the outer hair cells (OHCs) and inner hair cells (IHCs), but also caused dislocation of the hair cell rows. We hypothesized that the dislocation arose from damage to the support cells (SCs) that anchors hair cells within the epithelium. To test this hypothesis, rat postnatal cochlear cultures were treated with PQ. Shortly after PQ treatment, the rows of OHCs separated from one another and migrated radially away from IHCs suggesting loss of cell-cell adhesion that hold the hair cells in proper alignment. Hair cells dislocation was associated with extensive loss of SCs in the organ of Corti, loss of tympanic border cells (TBCs) beneath the basilar membrane, the early appearance of superoxide staining and caspase-8 labeling in SCs below the OHCs and disintegration of E-cadherin and β-catenin in the organ of Corti. Damage to the TBCs and SCs occurred prior to loss of OHC or IHC loss suggesting a form of detachment-induced apoptosis referred to as anoikis

Keywords

Paraquat; E-cadherin; β-catenin; caspase-8; superoxide; anoikis

Introduction

Paraquat is one of the most widely used organic herbicides (Shopova et al., 2007), but is highly toxic resulting in numerous fatalities worldwide (Dinis-Oliveira et al., 2008; Gawarammana and Buckley, 2011). Because of its toxicity, PQ has been banned in many

Corresponding author: Dalian Ding, Center for Hearing and Deafness, 137 Cary Hall, University at Buffalo, Buffalo, NY, USA; phone: 716 829 5311, fax: 716 829 2980; dding@buffalo.edu.

Declarations of interest: none

counties, although it is still employed in more than 130 developing countries resulting numerous poisonings over the past 20 years (Bertsias et al., 2004; Eddleston et al., 2002; Kavousi-Gharbi et al., 2017). PQ misuse has resulted in pollution of soil, water and agricultural products (Ikpesu, 2015; Li et al., 2016; Shopova et al., 2007). Long-term exposure to PQ has been linked to Parkinson's disease (Baltazar et al., 2014; Berry et al., 2010; Chen et al., 2010), pulmonary fibrosis, and skin cancer (Anderson and Scerri, 2003; Dinis-Oliveira et al., 2008; Jee et al., 1995; Sun et al., 2016; Wesseling et al., 2001). Because PQ concentrations in the lungs are 6–10 times higher than in plasma, cells in the lung are considered the primary target of PQ toxicity (Dinis-Oliveira et al., 2008). The high pulmonary concentration of PQ is linked to polyamine transporters, such as organic cation transporters that are abundantly expressed in membranes of alveolar and Clara cells (Dinis-Oliveira et al., 2008; Higashi et al., 2014; Ingoglia et al., 2015; Sala-Rabanal et al., 2013; Silva et al., 2015). PQ also accumulates in neurons by uptake through dopamine and organic cation transporters, leading to oxidative stress and neurotoxic symptoms resembling Parkinson's (Kuter et al., 2007; Rappold et al., 2011).

Because PQ is a potent superoxide generator, it has been used as a tool to investigate oxidative stress, cell death and otoprotection in the cochlea (Bielefeld et al., 2005; Nicotera et al., 2004). Treatment of cochlear organotypic cultures with 50 μM of PQ for 24 h resulted in significant loss of inner hair cells (IHCs) and outer hair cells (OHCs) and the magnitude of hair cell loss rose as the dose of PQ increased. PQ-induced hair cell loss was reduced significantly by M40403, a superoxide scavenger, consistent with previous studies showing that M40403 prevents PQ-induced neurotoxicity in substantia nigra (Mollace et al., 2003). When PQ was applied to the cochlea in vivo, it caused significant hearing loss over a broad range of frequencies and significant loss of OHCs and IHCs along the length of the cochlea (Bielefeld et al., 2005). Sound pre-conditioning, which increase the endogenous antioxidant enzymes in the cochlea, significant reduced PQ-induced hearing loss and IHC loss (Harris et al., 2006).

Although PQ-mediated cochlea damage is initiated by the overproduction of the superoxide radical, the cellular events that ultimately lead to hair cell death are poorly understood. In some tissues, PQ-induced cell death occurs through the caspase-9, intrinsic apoptotic pathway involving the release of cytochrome c from damaged mitochondria (Chen et al., 2012; Dinis-Oliveira et al., 2007a; Dinis-Oliveira et al., 2007b; Hong et al., 2013; Li et al., 2015a). In other cases, PQ-induced cell death is initiated through the caspase-8, extrinsic apoptotic pathway involving membrane damage (Hathaichoti et al., 2017; Wang et al., 2016). Currently, it is unclear if PQ-induced hair cell death is initiated through the intrinsic pathway involving permeabliization of the mitochondrial membrane and/or the extrinsic cell death pathway activated disruption of extracellular ligands that bind to cell-surface death receptors. When PQ was applied to cochlear organotypic cultures, it caused the orderly rows of hair cells to shift their position within the sensory epithelium prior to degenerating (Nicotera et al., 2004). The dislocation of the OHC rows suggested that PQ might disrupt the intercellular adhesion proteins that anchor the OHCs and IHCs to neighboring supporting cells (SCs). The cell adhesion molecules and intercellular connections also provide important signals for cell growth, cell fate, differentiation and survival (Kelley, 2003; Shi et al., 2014; Simonneau et al., 2003). Detachment of cells from their neighbors can trigger a

novel form of cell death known as anoikis; detachment-mediated apoptosis normally prevents cancer cells from metastasizing (Frisch and Ruoslahti, 1997; Frisch and Screaton, 2001; Liotta and Kohn, 2004; Reddig and Juliano, 2005; Valentijn et al., 2004). During embryogenesis, programmed cell death, cell detachment and anoikis play a role in cavity formation (i.e., cavitation) in some tissues (Boudreau et al., 1995; Coucouvanis and Martin, 1995; Qu et al., 2007); similar processes could conceivably contribute to the formation of large and moderate size fluid spaces in the cochlea. To determine if PQ-induced hair cell dislocation and death was triggered by disruption of intercellular connections, we treated cochlear organotypic cultures with PQ and evaluated extracellular matrix proteins and mechanisms of cell death in hair cells and supporting cells.

Materials and Methods

Subjects

Cochleae were obtained from postnatal day 3 (P3) Sprague-Dawley rat pups (Charles River Laboratories; Wilmington, MA). All experimental procedures were approved by the Institutional Animal Care and Use Committee (IACUC) at the University at Buffalo and conform to the National Institutes of Health guide for the care and use of Laboratory animals.

Cochlear organotypic cultures

Our procedures for preparing cochlear cultures have been described in our previous publications (Ding et al., 2002; Ding et al., 2011; Ding et al., 2013a; Li et al., 2015b; Prakash Krishnan Muthaiah et al., 2017{Yu, 2015 #67170; Yu et al., 2015)}. Briefly, a 9:1:1 mixture consisting of rat-tail collagen (Type 1, BD Biosciences, #4236, Bedford, MA), 10X basal medium eagle (Sigma B9638) and 2% sodium carbonate was freshly prepared and then 10 μl of the mixture was placed in the center of a 35 mm diameter culture dish (Falcon 1008, Becton Dickinson) for 30 minutes until the solution had gelled. Then 1.3 ml of serum-free medium [2 g bovine serum albumin (BSA, Sigma A-4919), 2 ml Serum-Free Supplement (Sigma I-1884), 4.8 ml of 20% glucose (Sigma G-2020), 0.4 ml penicillin G (Sigma P-3414), 2 ml of 200 mM glutamine (Sigma G-6392), and 190.8 ml of 1×BME (Sigma B-1522)] was added to the culture dish. The P3 rat pups were decapitated and their temporal bones carefully removed. In all cases, the entire cochlear basilar membrane, containing the organ of Corti and spiral ganglion neurons was carefully dissected out as a surface preparation in Hank's Balanced Salt Solution and placed on the surface of collagen gel in the culture dish. The lateral wall of the cochlea and Reissner's membrane were discarded. Both ears from each rat pup was used, but a different condition was applied to the genetically identical ear-pairs (e.g., 0 μM PQ vs. 200 μM PQ). Each experiment was repeated with ears from different litters of rat pups. Afterwards, the samples were placed in an incubator (Forma Scientific, #3029) and maintained at 37 °C in 5% CO_2 for one h after which an additional 0.7 ml of serum-free medium was added to the culture dish sufficient to cover the cochlear explants. Samples were maintained in the incubator overnight.

PQ Treatment

PQ was dissolved in serum-free medium. A stock solution was made for each experiment and diluted to the appropriate concentration. Cochlear explants were cultured in freshly prepared serum-free medium containing 0, 10, 50, 100, 200, or 500 μM of PQ (n = 6 cultures per concentration) for 24 h. Using PQ concentrations of 0, 50 or 200 μM applied to explants for 0, 6, 12 or 24 h, we also evaluated the expression of superoxide, caspase-8, caspase-9, and caspase-3 and immunolabeling of extracellular matrix proteins (n = 6 per condition).

Cochleograms

Cochlear explants were fixed with 10% formalin in PBS for 3 h. Specimens were stained with Alexa Fluor 555-labeled phalloidin (1:200, ThermoFisher Scientific A34055) for 1 h, mounted on glass slides in glycerin as flat surface preparations, cover slipped, and examined with a epifluorescence-equipped microscope (Zeiss Axioskop, 400X) with appropriate filters (absorption 555 nm, emission 565 nm). The numbers of IHCs and OHCs were counted over 0.24 mm intervals along the entire length of the cochlea. Hair cells were counted as missing if the stereocilia and cuticular plate were absent. Counts were entered into a custom computer program that computed a cochleogram showing the percent missing IHCs and OHCs as function of percent distance from the apex based lab hair cell norms for SASCO Sprague–Dawley rats (Ding et al., 2013a; Li et al., 2015b). Data from each individual cochleogram were averaged to generate a mean cochleogram for each experimental condition.

Semi-thin sections

Semi-thin plastic embedded sections were obtained from some cochlear explants that had been treated with 0 or 200 μM PQ for 6, 12 or 24 h using procedures described in our earlier publications (Ding et al., 1997a; Ding et al., 1997b; Ding et al., 2016; Wang et al., 1999). Afterwards the explants were fixed with 2.5% glutaraldehyde (EMS-16216) in PBS for 6 h. After rinsing with 0.1 M PBS, specimens were immersed in 2% osmium tetroxide in PBS for 2 h. The samples were dehydrated through a graded series of ethanol solutions ending with 100% and then embedded in Epon 812 resin. After polymerization, 3-μM plastic sections were obtained using an ultramicrotome (Leica Reichert Supernova) and placed on glass slides. Sections were stained with 0.1% toluidine blue solution for 1 minute and then coverslipped for observations under a light microscope.

Myosin VI and SOX2 Immunohistochemistry

Antibodies against myosin VI and SOX2 were used to identify hair cells and supporting cells respectively. Cochlear specimens were fixed for 1 h with 10% formalin in PBS and then rinsed three times with distilled water. To prevent non-specific labeling, specimens were incubated in 2% Triton X-100 and 5% donkey serum in 0.1 M PBS for 1 h at room temperature. Afterwards, the specimens were immersed overnight at 4 °C in 1% Triton X-100 and 5% donkey serum in 0.1 M PBS containing rabbit anti-myosin VI primary antibody (1:100, Sigma M5187) and goat anti-SOX2 primary antibody (1:100, Santa Cruz Biotechnology. Lot: L1708). Specimens were rinsed three times with PBS for 15 minutes

and incubated for 2 h at room temperature in donkey anti-rabbit secondary antibody conjugated with TRITC (1:200, Jackson ImmunoResearch, #72296) and donkey anti-goat secondary antibody conjugated with Alexa Fluor 488 (1:200, Invitrogen, #474685) in 1% Triton X-100 and 5% donkey serum in 0.1 M PBS. Nuclei were stained with To-Pro-3 (Life Technologies #T3605) during or after the process of secondary antibody labeling. Specimens were rinsed in PBS, mounted on glass slides in glycerin, coverslipped and examined with a confocal microscope (Zeiss LSM-510) with appropriate filters for TRITC (absorption: 544 nm, emission: 572 nm), Alex Fluor 488 (excitation 488 nm, emission 519 nm) or To-Pro-3 (excitation 642 nm, emission 661 nm). Multilayer images were evaluated with a Zeiss LSM Image Examiner, and post-processed with Adobe Photoshop software.

Superoxide detection

To detect superoxide, some cochlear cultures were incubated with dihydroethidium (DHE) (Sigma D7008). DHE is rapidly oxidized to fluorescent ethidium in the presence of superoxide after which ethidium preferentially binds to DNA (Deng et al., 2013; Ding et al., 2013a; Nicotera et al., 2004). Cochlear cultures were treated with 0 or 200 μM PQ for 6, 12 or 24 h and immediately afterwards incubated in serum-free medium containing 100 μM DHE for 1 h at 37 °C in a 5% CO_2 incubator. Afterwards, the explants were fixed with 10% formalin in PBS for 3 h. After rinsing in PBS, the specimens were stained with Alexa Fluor 488-conjugated phalloidin and To-Pro-3 to label the stereocilia and cuticular plate of hair cells and nuclei respectively.

E-Cadherin and β-Catenin Immunolabeling

Some cochlear cultures were immunolabeled with antibodies against E-cadherin and β-catenin in order to observe changes in the extracellular matrix and intercellular connections. Cochlear explants were fixed with 10% formalin for 1 h and then immersed in 2% Triton X-100 and 5% goat serum in 0.1 M PBS for 1 h at room temperature. Afterwards, the specimens were incubated overnight at 4 °C in 1% Triton X-100 and 5% goat serum in 0.1 M PBS containing a mouse anti-E-cadherin monoclonal primary antibody (1:100, Cell Signaling Technology, #9562S) or a rabbit anti-β-catenin monoclonal primary antibody (1:100, Cell Signaling Technology, #14472S). After rinsing 3X in 0.1 M PBS, specimens were incubated for 2 h at room temperature in a goat anti-mouse secondary antibody conjugated with Alexa Fluor 488 (1:200, Invitrogen, #482679) or goat anti-rabbit secondary antibody conjugated with TRITC (1:200, Abcam, AB6718). To label the stereocilia and cuticular plate of hair cells, specimens were stained for 1 h with TRITC-labeled phalloidin (1:200, Sigma P1951) or Alexa 488-conjugated phalloidin (1:200, Molecular Probes A12379). Cell nuclei were labeled with To-Pro-3 for 1 h (1: 100, Life technologies, #T3605). Specimens were mounted on glass slides in glycerin, cover slipped, and examined under confocal microscope with appropriate filters as described previously (Liu et al., 2014; Prakash Krishnan Muthaiah et al., 2017).

Caspase Labeling

Some cultures were labeled with cell permeable carboxyfluorescein probes that recognizes activated caspase-3, -8, or -9 (CaspGLOW Red Active (BioVision); labeling was carried out according to the manufacturer’s instructions (Deng et al., 2013; Ding et al., 2013a; Li et al.,

2015b). At the end of the experimental treatments, the explants were incubated with one of the above probes at a dilution of 1:100 for 1 h. Afterwards, the specimens were fixed in 10% formalin in PBS for 3 h, and stained with Alexa Fluor 488-conjugated phalloidin and To-Pro-3 to label the stereocilia and cuticular plate of the hair cells and the nuclei respectively. Afterwards, the specimens were mounted in glycerin on glass slides, cover slipped and examined with a confocal microscope with appropriate filters.

E-Cadherin and β-Catenin Western blots

Western blotting was used to assess the expression of β-catenin and E-cadherin in cochlear explants treated with 0 or 200 μM PQ for 6, 12 or 24 h. Afterwards, the cochlear explants were harvested and immersed in 100 μl RIPA (Radioimmunoprecipitation) Lysis Buffer System following the manufacturer's instructions. (Santa Cruz, SC24948). Protein concentrations were quantified using a BCA Protein Assay Kit (Pierce, 23227). Equal quantities of protein from each experimental condition were separated by 7.5% sodium dodecyl sulfate polyacrylamide gel electrophoresis (30% Acrlamide/Bis 7.5 ml; 1.5 M Tris-HCL pH 8.8, 7.5 ml; DDW 14.4 ml; 10% SDS 0.3 ml; 10% APS 0.3 μl, TEMED 30 μl, total volume 30 ml). Separated proteins were transferred onto pure nitrocellulose blotting membranes (Sigma, N8017) and blocked overnight with 5% skimmed milk. E-cadherin (Cell Signaling Technology, #9562S, 1:1000) or β-catenin (Cell Signaling Technologies, #14472S, 1:1000) monoclonal antibodies and β-actin (Sigma, 1:10000) were applied to the membranes for 12 h with shaking. Afterwards, the membranes were washed three times with PBS with Tween 20. Each membrane was incubated for 2 h at room temperature on a shaker with an alkaline phosphatase-conjugated goat anti-mouse secondary antibody (Novus Biologicals, USA, NBP1-72574, 1:5000) or goat anti-rabbit secondary antibody (Novus Biologicals, USA; NBP1-75294, 1:5000). Membranes were then washed with 0.1 PBS with Tween 20 three times. Label was detected with a BCIP/NBT substrate detection Kit (Genemed Biotechnologies, Inc., CA, USA, 10-0007) following the manufacturer's instructions. Samples were run in triplicate and the intensity of the bands was quantified using ImageJ (1.46J) software (Ding et al., 2013b; He et al., 2011; Zhang et al., 2003).

Statistical Analysis

Statistical analyses were carried out with GraphPad Prism software (GraphPad Software, USA) using a one-way ANOVA with Bonferroni or Newman-Keuls post-hoc testing ($p<0.05$) as described in more detail in the Results section.

Results

Hair Cell Loss

Mean (n=6) cochleograms showing the percent IHC and OHC loss as a function of percent distance from the apex of the cochlear are shown in Figure 1 after 24 h treatment with 0, 10, 50, 100, 200 and 500 μM PQ. There was little hair cell loss in the control condition (0 μM PQ) except near the base of the cochlea (80–100%) where some mechanical damage typically occurred during sample preparation (Figure 1A). As the dose of PQ increased from 10 to 500 μM PQ, the hair cell lesions increased and spread from the base (100% location) toward the apex (0% location). OHC losses were greater than IHC losses (Figure 1B–F),

consistent with most ototoxic drugs (Ding et al., 2012; Forge and Schacht, 2000). The mean (+SEM, n = 6 cochlea per condition) numbers of OHCs/mm (Figure 1G) and IHCs/mm (Figure 1H) were computed over the length of the cochlea for each experimental condition. OHC densities in cultures treated with 10–500 μM PQ were significantly less than control explants (0 μM PQ); OHC densities for neighboring PQ concentrations were significantly different from one another (Figure 1G) (one-way ANOVA, $F= 128.2$, 5, 30 df, $p<0.0001$; Newman-Keuls post-hoc $p<0.05$). IHC densities from PQ treatments from 100 to 500 μM were significantly less than controls (0 μM PQ) and IHC densities at 500 μM PQ were significantly less than 200 μM PQ (Figure 1H) (one-way ANOVA, $F= 15.31$, 5, 30 df, $p<0.0001$; Newman-Keuls post-hoc $p<0.05$). These results are consistent with our previous studies of PQ ototoxicity (Nicotera et al., 2004).

Hair Cell Dislocation

Figure 2A–G shows a series of representative confocal images of cochlear surface preparations in which the stereocilia and cuticular plate of the IHCs and OHCs were labeled with TRITC-conjugated phalloidin. The three rows of OHCs and single row of IHCs were arranged in orderly rows in the (A) control group (0 μM PQ) and (B) the group treated with 10 μM PQ for 24 h. However, 24 h treatment with 50 μM PQ (C) resulted in severe dislocation of the three rows of OHC with the second and third row of OHCs shifting radially away from the IHCs. The hair cells rows were distorted and scalloped and many OHCs were missing. As the PQ dose increased from 100 to 500 μM (Figure 2E–G), the hair cells rows became more distorted and hair cell losses increased. The distorted hair cell rows and the radial-shift in the location of the OHCs suggested the PQ might be damaging the SCs that help to maintain the highly structured architecture of the epithelium.

Time Course

The time course of damage was evaluated in more detail by obtaining 3 μM radial sections from cultures treated with 200 μM PQ for 6, 12 or 24 h and comparing them to untreated controls (0 μM PQ) cultured for 24 h. In controls, a single row of IHCs was present alongside the inner pillar cells (PC) and three rows of OHCs, which rested above the Deiters cells (DC). Several layers of cells, possibly mesothelial cells (Keithley et al., 1993), were present beneath the basilar membrane (Figure 3A, dashed line); these cells known as tympanic border cells (TBCs) sometimes serve as progenitor cells in the developing cochlea (Jan et al., 2013). After 6-h treatment with 200 μM PQ, the OHCs, IHCs, and DCs were still present. However, many nuclei were shrunken or condensed in the TBCs beneath the BM (Figure 3B). Some DC nuclei were shrunken and condensed. At 12 h post-PQ, the IHCs and OHCs were still present; however, most of the DCs beneath the OHCs were missing. Most TBCs beneath the BM were absent, but the nucleus in those still present was condensed or fragmented (Figure 3C). After 24-h treatment with 200 μM PQ, many hair cells were missing and all the DCs were absent. The soma of the remaining hair cells were shrunken and the nucleus was condensed (Figure 3D). Most TBCs beneath the basilar membrane were missing. Taken together, these results indicate that damage to the TBCs and DCs occurs 6–12 h before there is significant hair cell loss.

Early Supporting Cell Destruction

We used antibodies against myosin VI and SOX2 to label hair cells and SCs respectively in PQ-treated cultures and To-Pro-3 to label nuclei. In untreated controls cultured for 24 h, three rows of OHCs and one row of IHCs were evident when the confocal image stack was viewed from the surface of the organ of Corti (Figure 4A2). In this surface-view of the image stack, the turquoise, SOX2-labeled SCs partially mask the red, myosin VI-labeled hair cells. There is a high density of SOX2-labeled SCs in the inner sulcus cell (ISC) region medial to the IHCs. In the Z-plane confocal cross section through the image stack, the red, myosin VI-labeled OHCs with blue, To-Pro-3 nuclei are perched above the turquoise, SOX2-labeled DCs. A SOX-2-labeled Hensen cell (HC) lies lateral to outermost OHC and a SOX-2-labeled outer PC lies medial to the innermost OHC (Figure 4A1). A red, myosin VI-labeled IHC lies above an inner PC.

Treatment of cochlear explants with 200 μM PQ for 6 h damaged many SCs. The loss of turquoise SCs in the confocal image stack unmasked the red OHCs, now arranged in somewhat irregular rows (Figure 4B2, red arrows). The Z-plan confocal image (Figure 4B1) revealed a paucity of turquoise-labeled SCs as well as missing DCs beneath the OHCs and missing PC beneath the IHC. Fewer SCs were present in the ISC region compared to controls (Figure 4B1, B2). After 12 h treatment with 200 μM PQ (Figure 4C1, C2), red-myosin VI OHCs and IHCs were still present, but many HCs, DCs, PCs and ISCs were missing. After 24 h treatment with 200 μM PQ, nearly all the OHCs and surrounding support cells (i.e., HC, DCs and OPCs) were missing; however, most IHCs, inner PCs and ISCs were present (Figure 4C1, C2). These results indicate that the DCs, HCs and outer PCs are more susceptible to PQ damage than the OHC and IHCs.

PQ-induced superoxide

DHE, which is oxidized to fluorescent ethidium in the presence of superoxide, was used to identify sites of superoxide generation in PQ-treated explants. In normal, untreated cochlear explants, DHE staining was largely undetectable (Figure 5A); however, after 6 h treatment with 200 μM PQ treatment, DHE fluorescence was mainly seen in the indicated SC layer mostly in cells beneath the basilar membrane (Figure 5B). When the duration of treatment with 200 μM PQ was increased to 12 h, DHE fluorescence increased and spread to many cells in the indicated SC layer as well as a few OHCs and IHCs (Figure 5C). After 24-h treatment with 200 μM PQ, most cells in the indicated SC layer had disappeared; consequently, DHE fluorescence was mainly observed in the hair cells (Figure 5D). To quantify the temporal sequence of superoxide generation in the SC layer and hair cell layer, we measured the DHE levels in both cells types before and 6, 12 and 24 h after PQ treatment. DHE levels were low in control explants and there was no difference between labeling in the SC layer and hair cell layer (Figure 5E). However, DHE levels were significantly higher in the SC layer than the hair cell layer 6 h and 12 h after treatment with 200 μM PQ, whereas after 24 h treatment, DHE levels were much higher in the hair cell layer than the SC layer (one-way ANOVA, $F= 231.5$; 3, 1 df, $p<0.0001$, Bonferroni post-hoc test, $p<0.05$).

PQ-induced caspases

To identify cell death signaling pathways involved in PQ damage, explants were labeled with flurogenic probes that recognize activated initiator caspase-8, initiator caspase-9 or executioner caspase-3. Samples were evaluated from normal explants and explants treated for 6, 12 or 24 h with 200 μM PQ. Representative confocal images were taken from the OHC layer near the surface of the organ of Corti and a region referred to as the DC layer that included DCs and slightly deeper layers of the organ of Corti. Caspase-3, -8 and -9 were largely undetectable in the OHC layer and the DC layer in untreated controls cultured for 24 h (Figure 6A1, B1 and C1). After 6 h treatments with 200 μM PQ, caspase-8 appeared mainly in the DC layer (Figure 6A2). Caspase-9 labeling was absent from the OHC layer and DC layer (Figure 6B2). Caspase-3 labeling was absent from the OHC layer (Figure 6Ca, but was beginning to be expressed in the DC layer (Figure 6Cb). After 12 h treatment with 200 μM PQ, caspase-8 was expressed widely in the DC layer (Figure 6A2b), but was absent from the OHC layer (Figure 6A3) (Figure 6A3). Caspase-9 was absent from the OHC layer (Figure 6B3a), but was beginning to emerge in the DC layer after 12 h of PQ treatment whereas caspase-3 was heavily expressed in the DC layer (Figure 6B3b) and just detectable in a few cells in the OHC layer (Figure 6B3a). After 24 h of PQ treatment, many cells in the OHC layer and SC layer had already degenerated. Consequently, caspase-8, -9 and -3 labeling was patchy or marginally present in the OHC layer and DC layer (Figure 3A4, B4, C4). To quantify the results, we counted the numbers of caspase-8, -9 and -3 positive cells located in the OHC layer and DC layer in confocal images taken from the middle of the cochlea in controls explants cultured for 24 h (Cnt) and explants treated with 200 mM PQ for 6, 12 or 24 h. Counts were obtained from five organotypic cultures for each condition using confocal images similar to those in Figure 6A–C and the mean numbers (+/− SD) plotted in Figure 6D–F. The numbers of caspase-8 cells in the DC layer increased from zero in controls to approximately 40 and then 60 after 6 h and 12 h PQ treatment, but after 24 h PQ treatment, the number approached zero due considerable cell death in this layer (Figure 6D). In contrast, the numbers of caspase-8 labeled cells in the OHC layer increased slowly from near zero in controls to approximately 20 after 24 h PQ treatment. Caspase-3 counts in the DC layer and OHC layer followed a similar temporal progression as that for caspase-8 during the 6 to 24 h of PQ treatment (Figure 6F). The temporal progression of caspase-9 counts in the OHC layer and DC layer followed a similar pattern to that for caspase-8 and caspase-3 except that upsurge of caspase-9 in the DC layer was delayed by approximately 6 h (Figure 6E).

PQ suppresses β-catenin and E-cadherin

E-cadherin, a cell-cell adhesion protein and β-catenin, which coordinates cell-cell adhesion, can be disrupted by cochlear damage (Leonova and Raphael, 1997; Mahendrasingam et al., 1997; Warchol, 2007; Whitlon, 1993). Because the OHC rows were distorted and separated from the IHCs after PQ treatment, we speculated that E-cadherin and β-catenin immunolabeling patterns would be disrupted prior to hair cell degeneration. To test this hypothesis, we immunolabeled cochlear explants from 6 to 24 h after PQ treatment. In control explants cultured for 24 h without PQ, we observed strong green E-cadherin labeling around the circumference of the phalloidin-labeled (red/orange) OHCs and IHCs in confocal images localized to the hair cell layer of the epithelium (Figure 7A). Confocal images taken

at the SC layer below the hair cells revealed thin, green circumferential rings of E-cadherin at the intercellular boundaries (Figure 7E). After 6 h treatment with 200 μM PQ, the E-cadherin rings around the SCs developed a fuzzy, discontinuous and crenulated appearance suggesting a loss of intercellular contact (Figure 1F) whereas E-cadherin labeling encircling the hair cells appeared normal (Figure 7B). After 12 h treatment with 200 μM PQ, the rings of E-cadherin had largely disappeared in the SC layer (Figure 7G) whereas E-cadherin and myosin VI labeling in the hair cell layer appeared normal (Figure 7C). However, after 24 h of PQ treatment only E-cadherin puncta were visible in the SC layer (Figure 7H). In the hair cells layer, E-cadherin was greatly reduced, most OHCs were missing while the row of IHCs was irregular and some IHCs were missing (Figure 7D). Thus, E-cadherin labeling was initially disrupted in the SC layer after 6 h of PQ treatment and by 12 h it was greatly reduced whereas E-cadherin in the hair cell layer remained intact.

In control explants, robust green β-catenin labeling was present in the circumference of the phalloidin-labeled (red/orange) OHCs and IHCs (Figure 7I). In the SC layer, thin, green rings of β-catenin were present at the intercellular boundaries of the SCs (Figure 7E). After 6 h treatment with 200 μM PQ, β-catenin labeling in the SC layer appeared normal (Figure 7N). However, after 12 h of PQ treatment, β-catenin declined dramatically in the SC layer (Figure 7O) while β-catenin around the IHCs and OHCs was normal (Figure 7K). After 24 h of PQ treatment, β-catenin had disappeared from large section of the SC layer (Figure 7L) and hair cell layer (Figure 7L) in regions of OHC loss even though some OHC were still present. The decline in β-catenin in the SC layer, like the decline in E-cadherin, occurred prior to hair cells loss.

Using Western blots, we compared the expression of E-cadherin and β-catenin proteins relative to β-actin in control explants cultured for 24 h and explants treated with 200 μM PQ for 6, 12 or 24 h. The expression of the E-cadherin band with a molecular weight around 135 kDa, was greatly reduced 12 and 24 h after treatment with 200 μM PQ while the band of β-actin remained stable (Figure 8A). The mean (n = 3 replicates, SEM) expression of E-cadherin relative to β-actin was significantly less than controls 12 h and 24 h after 200 μM PQ treatment (Figure 8B) (one-way ANOVA, $F= 98.2, 3, 8$ df, $p<0.001$, Newman-Keuls post-hoc, $p<0.05$), consistent with E-cadherin immunolabeling. Western blots of β-catenin revealed a prominent band around 92 kDa that declined noticeably 12 and 24 h after 200 μM PQ whereas β-actin remained stable (Figure 8C). The mean (n = 3 replicates, SEM) expression of β-catenin relative to β-actin was significantly less than controls 12 h and 24 h after 200 μM PQ treatment (Figure 8D) (one-way ANOVA, $F= 125.3, 3, 8$ df, $p<0.001$, Newman-Keuls post-hoc, $p<0.05$), consistent with β-catenin immunolabeling.

Discussion

The hair cell lesions induced by PQ spread from base to apex in a dose-dependent manner and the loss of OHCs was greater than IHCs, a pattern similar to that seen with other ototoxic drugs (Forge et al., 2000; Nicotera et al., 2004; Rybak and Ramkumar, 2007). As the lesion developed, the OHC rows separated and migrated radially suggesting the loss of intercellular attachments. OHC dislocation was first observed 6 h after PQ treatment in synchrony with the loss of SCs and TBCs beneath the basilar membrane (Figure 3B); these

changes were associated with an increase in DHE fluorescence in the SC layer (Figure 5B, E), enhanced expression of initiator caspase-8 (Figure 6D) and executioner caspase-3 (Figure 6F) in the DC layer and mild disruption of the E-cadherin surrounding the SCs (Figure 7F). After 12 h of PQ treatment, shrinkage and loss of DCs, HCs and TBCs appeared beneath the hair cells (Figure 3C); these changes were accompanied by increased expression of caspase-8 (Figure 6D) and caspase-3 (Figure 6F) in the DC layer, and loss of E-cadherin (Figure 7G) and β-catenin (Figure 7O) in the SC layer. Only after the TBCs, DCs and HCs, did the OHCs and IHCs begin to die off.

Trigger Points

Our analysis revealed a temporal-spatial progression of superoxide-induced DHE fluorescence. DHE labeling first appeared in TBCs and some SCs after 6 h of PQ treatment; after 12 h of PQ treatment, fluorescence appeared around the DC layer and after 24 h, DHE labeling reached the hair cells at the surface of the epithelium (Figure 5). Expression of initiator caspase-8 and caspase-3 followed a similar temporal-spatial progression (Figure 6D, F) while the appearance of caspase-9 (Figure 6E) was slightly delayed. The mechanisms regulating the temporal-spatial progression of superoxide expression are unclear. One factor likely to play a role is the relative abundance of protective superoxide dismutase enzymes that inactivate the toxic superoxide anion. *In vivo*, Cu/Zn superoxide dismutase is more abundant in the cytoplasm of brain astrocytes than in neurons whereas manganese superoxide dismutase is more abundant in neurons than glia (Lindenau et al., 2000). The relative abundance of these antioxidant enzymes changes *in vitro*. In primary cortical cultures, Cu/Zn superoxide dismutase is expressed at similar levels in neurons and astrocytes whereas Mn superoxide dismutase is most strongly expressed in microglia. The spatial-temporal distribution of superoxide dismutase enzymes also changes during development (Yon et al., 2008). The distribution of superoxide dismutase enzymes has not been determined in postnatal cochlear explants, but based on the progression of DHE fluorescence, the abundance of superoxide dismutase enzymes would be expected to be lowest in the TBCs underneath the basilar membrane and higher in the hair cell layer.

One of the earliest sites of damage occurred in the TBCs beneath the basilar membrane, a region where resident macrophages are also present (Frye et al., 2017; Yang et al., 2015). It is conceivable that PQ-induced damage to the TBCs results in the activation of the resident macrophages which in turn leads to the release of superoxide or other toxic free radicals that serve to further amplify damage to TBC and surrounding SCs in the organ of Corti (Assreuy et al., 1994; Mosser and Edwards, 2008). To determine which cells types are especially vulnerable to PQ toxicity, it would be necessary to label the various cell types beneath the hair cells with antibodies unique to each cellular subpopulation. Such an endeavor would be challenging given that protein expression patterns are likely to changes substantially during postnatal development.

Connections

E-cadherin and β-catenin play important roles in forming adherens junctions and cell-cell connections that help to establish the complex architecture of the cochlea (Gumbiner, 1995; Kuo et al., 2015; Shi et al., 2014; Simonneau et al., 2003; Takeichi, 1995) and re-establish

the intercellular junctions needed to maintain the ionic barrier at the reticular lamina following hair cell loss (Leonova et al., 1997). In P3 cochlear explants, E-cadherin and β-catenin surrounded the hair cell cuticular plate near the surface of the epithelium. In the DC layer below the OHCs, E-cadherin and β-catenin were present at the intercellular boundaries of adjacent SCs (Figure 7), consistent with previous reports (Leonova et al., 1997; Whitlon, 1993). After 6 h PQ treatment, E-cadherin labeling became discontinuous, beaded and crenulated (Figure 7F, arrowheads), signs that the DCs and SCs were losing contact with one another, disrupting cell-cell contacts and intercellular communication. One possible interpretation of these results is that PQ might directly damage E-cadherin proteins. Alternatively, it is conceivable that PQ initially damaged the DC leading to secondary changes in E-cadherin. Future experiments are needed to distinguish between these possibilities. After 12 h of PQ treatment, labeling of E-cadherin and β-catenin was largely absent from the DC region but persisted in the OHC layer (Figure 7C, G, K and O). The changes in E-cadherin and β-catenin may ultimately set the stage for subsequent scar formation. OHC losses only occurred after E-cadherin and β-catenin had disappeared from the apical surface of the epithelium (Figure 7D, L). One possible interpretation of these results is that the loss of intercellular connections between hair cells and DCs leads to a form of cell death known as anoikis, or detachment apoptosis (Boudreau and Jones, 1999; Frisch et al., 2001; Taddei et al., 2012) as seen in PQ-treated alveolar epithelial cells (Dinis-Oliveira et al., 2008). An alternative possibility for the temporal sequence of cell death is that TBCs and SCs are simply more vulnerable to PQ than hair cells because of differences in their antioxidant enzymes or the unique nature of PQ toxicity. Additional experiments are needed to confirm or reject the hypothesis that PQ-induced hair cell death occurs by anoikis.

Early Activation of Caspase-8

A cell's ability to resist cell detachment from its neighbors is critical to preventing anoikis (Eccles and Welch, 2007). PQ decreases E-cadherin expression (Yamada et al., 2015). Among intestinal enterocytes, loss of E-cadherin leads to anoikis (Fouquet et al., 2004). Similarly, COX-2 inhibitors, which downregulate β-catenin and E-cadherin, induce anoikis in osteosarcoma cells (Liu et al., 2012). Anoikis manifests all the features of apoptosis such as caspase activation and nuclear fragmentation and condensation (Frisch et al., 2001; Reddig et al., 2005). Caspase-9 mediated cell death is initiated by the release of cytochrome c from the mitochondria followed by activation of apaf-1 and cleavage of the inactive zymogen into its active form leading to downstream activation of executioner caspase-3 (Budihardjo et al., 1999; Takatani et al., 2004). Initiator caspase-8 is activated by extracellular ligands such as FAS that bind to death receptors forming a death inducing signaling complex (DISC) (Budihardjo et al., 1999; Hathaichoti et al., 2017). Disruption of cell-cell contacts required for intercellular communication activates caspase-8 leading to direct activation of executioner caspase-3 or indirect activation of caspase-3 through the intrinsic mitochondrial pathway (Park et al., 1999; Rytomaa et al., 1999). PQ activated both the extrinsic and intrinsic apoptotic pathways, however, activation of caspase-8 occurred much earlier than caspase-9. Thus, our results suggest that the decreased expression of E-cadherin and β-catenin that occurs soon after PQ treatment disrupts cell-cell contacts which may initiate detachment apoptosis (Bozzo et al., 2006; Fouquet et al., 2004; Stupack et al., 2001).

Reactive oxygen species (ROS) contribute to cochlear pathologies induced by ototoxic drugs, neurotoxic metals and intense noise, but the extent to which ROS disrupts cell-cell contacts that could initiate anoikis is poorly understood (Ding et al., 2012; Nicotera et al., 2004; Salvi et al., 2002; Samson et al., 2008). Preliminary studies currently underway in our lab suggest that certain ototoxic drugs, such as aminoglycosides, seem to preferentially damage hair cells, but not SCs or TBCs while other ototoxic agents damage both hair cells and SC. In other tissues, ROS suppress cell adhesion and promote anoikis (Cai et al., 2008; Chang et al., 2013; Chiarugi and Giannoni, 2008; Lin et al., 2011; Pani et al., 2009; Paoli et al., 2013). However, metastatic tumor cells can escape detachment apoptosis by circumventing ROS-induced oxidative stress (Lu et al., 2015).

SC and TBC loss and regeneration

Damaged mammalian hair cells do not regenerate. However, there is growing awareness that SCs and TBCs can differentiate into new hair cells if the required signals are applied at the appropriate time (Jan et al., 2013; Zheng and Gao, 2000). In the avian cochlea where hair cells naturally regenerate, loss of contact inhibition mediated by E-cadherin and β-catenin, key signals in the wnt pathway, promote the transdifferentiation of SCs to hair cells (Warchol, 2002). In mammals, inhibitors of γ-secretase cause postnatal utricular SCs to internalize their E-cadherin. Afterwards, the SCs begin to express hair cell markers such *Atoh1*, myosin VI and VIIa and form hair bundles. However, transdifferentiation ceases at postnatal day16 (Collado et al., 2011). In the mature cochlea, γ-secretase inhibitors blocks notch signaling that normally prevents SCs from transdifferentiating into hair cells (Mizutari et al., 2013; Tona et al., 2014). In the noise-damaged mammalian cochlea, γ-secretase inhibitors enhanced transdifferentiation of SCs into hair cells and aided the recovery of hearing. However, this interpretation is complicated by the fact that some γ-secretase inhibitors such as MDL28170 block calcium-activated proteases and promote hair cell survival (Lanzoni et al., 2005; Tona et al., 2014). While transdifferentiation of SCs appears to be a promising approach to restoring hearing, our results suggest that PQ or other ototraumatic agents that destroy SCs and TBC would prevent transdifferentiation and also interfere with scar formation and repair of the sensory epithelium (Leonova et al., 1997).

Supplementary Material

Refer to Web version on PubMed Central for supplementary material.

Acknowledgments

Research supported in part by NIH (R01DC011808, R01DC014452 and R01DC014693)

References

Anderson KD, Scerri GV. A case of multiple skin cancers after occupational exposure to pesticides. Br J Dermatol. 2003; 149:1088–9. [PubMed: 14632830]

Assreuy J, Cunha FQ, Epperlein M, Noronha-Dutra A, O'Donnell CA, Liew FY, Moncada S. Production of nitric oxide and superoxide by activated macrophages and killing of Leishmania major. Eur J Immunol. 1994; 24:672–6. [PubMed: 8125136]

Baltazar MT, Dinis-Oliveira RJ, de Lourdes Bastos M, Tsatsakis AM, Duarte JA, Carvalho F. Pesticides exposure as etiological factors of Parkinson's disease and other neurodegenerative diseases–a mechanistic approach. Toxicol Lett. 2014; 230:85–103. [PubMed: 24503016]

Berry C, La Vecchia C, Nicotera P. Paraquat and Parkinson's disease. Cell Death Differ. 2010; 17:1115–25. [PubMed: 20094060]

Bertsias GK, Katonis P, Tzanakakis G, Tsatsakis AM. Review of clinical and toxicological features of acute pesticide poisonings in Crete (Greece) during the period 1991-2001. Med Sci Monit. 2004; 10:CR622–7. [PubMed: 15507854]

Bielefeld EC, Hu BH, Harris KC, Henderson D. Damage and threshold shift resulting from cochlear exposure to paraquat-generated superoxide. Hear Res. 2005; 207:35–42. [PubMed: 15935579]

Boudreau N, Sympson CJ, Werb Z, Bissell MJ. Suppression of ICE and apoptosis in mammary epithelial cells by extracellular matrix. Science. 1995; 267:891–3. [PubMed: 7531366]

Boudreau NJ, Jones PL. Extracellular matrix and integrin signalling: the shape of things to come. Biochem J. 1999; 339(Pt 3):481–8. [PubMed: 10215583]

Bozzo C, Sabbatini M, Tiberio R, Piffanelli V, Santoro C, Cannas M. Activation of caspase-8 triggers anoikis in human neuroblastoma cells. Neurosci Res. 2006; 56:145–53. [PubMed: 16872704]

Budihardjo I, Oliver H, Lutter M, Luo X, Wang X. Biochemical pathways of caspase activation during apoptosis. Annu Rev Cell Dev Biol. 1999; 15:269–90. [PubMed: 10611963]

Cai J, Niu X, Chen Y, Hu Q, Shi G, Wu H, Wang J, Yi J. Emodin-induced generation of reactive oxygen species inhibits RhoA activation to sensitize gastric carcinoma cells to anoikis. Neoplasia. 2008; 10:41–51. [PubMed: 18231637]

Chang W, Song BW, Moon JY, Cha MJ, Ham O, Lee SY, Choi E, Choi E, Hwang KC. Anti-death strategies against oxidative stress in grafted mesenchymal stem cells. Histol Histopathol. 2013; 28:1529–36. [PubMed: 23760682]

Chen Q, Niu Y, Zhang R, Guo H, Gao Y, Li Y, Liu R. The toxic influence of paraquat on hippocampus of mice: involvement of oxidative stress. Neurotoxicology. 2010; 31:310–6. [PubMed: 20211647]

Chen YW, Yang YT, Hung DZ, Su CC, Chen KL. Paraquat induces lung alveolar epithelial cell apoptosis via Nrf-2-regulated mitochondrial dysfunction and ER stress. Arch Toxicol. 2012; 86:1547–58. [PubMed: 22678742]

Chiarugi P, Giannoni E. Anoikis: a necessary death program for anchorage-dependent cells. Biochem Pharmacol. 2008; 76:1352–64. [PubMed: 18708031]

Collado MS, Thiede BR, Baker W, Askew C, Igbani LM, Corwin JT. The postnatal accumulation of junctional E-cadherin is inversely correlated with the capacity for supporting cells to convert directly into sensory hair cells in mammalian balance organs. J Neurosci. 2011; 31:11855–66. [PubMed: 21849546]

Coucouvanis E, Martin GR. Signals for death and survival: a two-step mechanism for cavitation in the vertebrate embryo. Cell. 1995; 83:279–87. [PubMed: 7585945]

Deng L, Ding D, Su J, Manohar S, Salvi R. Salicylate Selectively Kills Cochlear Spiral Ganglion Neurons by Paradoxically Up-regulating Superoxide. Neurotox Res. 2013

Ding D, Wang J, Salvi RJ. Early damage in the chinchilla vestibular sensory epithelium from carboplatin. Audiol Neurootol. 1997a; 2:155–67. [PubMed: 9390829]

Ding D, Stracher A, Salvi RJ. Leupeptin protects cochlear and vestibular hair cells from gentamicin ototoxicity. Hear Res. 2002; 164:115–26. [PubMed: 11950531]

Ding D, Allman BL, Salvi R. Review: ototoxic characteristics of platinum antitumor drugs. Anat Rec (Hoboken). 2012; 295:1851–67. [PubMed: 23044998]

Ding D, Zheng X, Wang J, Hofstetter P, Salvi RJ. Quantitative analysis of nerve fibers in habenula perforata in chinchilla. Chinese Journal of Otolaryngology. 1997b

Ding D, He J, Allman BL, Yu D, Jiang H, Seigel GM, Salvi RJ. Cisplatin ototoxicity in rat cochlear organotypic cultures. Hear Res. 2011; 282:196–203. [PubMed: 21854840]

Ding D, Jiang H, Chen GD, Longo-Guess C, Muthaiah VP, Tian C, Sheppard A, Salvi R, Johnson KR. N-acetyl-cysteine prevents age-related hearing loss and the progressive loss of inner hair cells in gamma-glutamyl transferase 1 deficient mice. Aging (Albany NY). 2016; 8:730–50. [PubMed: 26977590]

Ding D, Qi W, Yu D, Jiang H, Han C, Katsuno K, Hsieh Y, Miyakawa T, Salvi R, Tanokura M, Someya S. NAD+ prevents mefloquine-induced neuroaxonal and hair cell degeneration through reduction of caspase-3-mediated apoptosis. PLoS One. 2013a

Ding D, Qi W, Yu D, Jiang H, Han C, Kim MJ, Katsuno K, Hsieh YH, Miyakawa T, Salvi R, Tanokura M, Someya S. Addition of exogenous NAD+ prevents mefloquine-induced neuroaxonal and hair cell degeneration through reduction of caspase-3-mediated apoptosis in cochlear organotypic cultures. PLoS One. 2013b; 8:e79817. [PubMed: 24223197]

Dinis-Oliveira RJ, Duarte JA, Sanchez-Navarro A, Remiao F, Bastos ML, Carvalho F. Paraquat poisonings: mechanisms of lung toxicity, clinical features, and treatment. Crit Rev Toxicol. 2008; 38:13–71. [PubMed: 18161502]

Dinis-Oliveira RJ, Sousa C, Remiao F, Duarte JA, Navarro AS, Bastos ML, Carvalho F. Full survival of paraquat-exposed rats after treatment with sodium salicylate. Free Radic Biol Med. 2007a; 42:1017–28. [PubMed: 17349929]

Dinis-Oliveira RJ, Sousa C, Remiao F, Duarte JA, Ferreira R, Sanchez Navarro A, Bastos ML, Carvalho F. Sodium salicylate prevents paraquat-induced apoptosis in the rat lung. Free Radic Biol Med. 2007b; 43:48–61. [PubMed: 17561093]

Eccles SA, Welch DR. Metastasis: recent discoveries and novel treatment strategies. Lancet. 2007; 369:1742–57. [PubMed: 17512859]

Eddleston M, Karalliedde L, Buckley N, Fernando R, Hutchinson G, Isbister G, Konradsen F, Murray D, Piola JC, Senanayake N, Sheriff R, Singh S, Siwach SB, Smit L. Pesticide poisoning in the developing world–a minimum pesticides list. Lancet. 2002; 360:1163–7. [PubMed: 12387969]

Forge A, Schacht J. Aminoglycoside antibiotics. Audiol Neurootol. 2000; 5:3–22. [PubMed: 10686428]

Fouquet S, Lugo-Martinez VH, Faussat AM, Renaud F, Cardot P, Chambaz J, Pincon-Raymond M, Thenet S. Early loss of E-cadherin from cell-cell contacts is involved in the onset of Anoikis in enterocytes. J Biol Chem. 2004; 279:43061–9. [PubMed: 15292248]

Frisch SM, Ruoslahti E. Integrins and anoikis. Curr Opin Cell Biol. 1997; 9:701–6. [PubMed: 9330874]

Frisch SM, Screaton RA. Anoikis mechanisms. Curr Opin Cell Biol. 2001; 13:555–62. [PubMed: 11544023]

Frye MD, Yang W, Zhang C, Xiong B, Hu BH. Dynamic activation of basilar membrane macrophages in response to chronic sensory cell degeneration in aging mouse cochleae. Hear Res. 2017; 344:125–134. [PubMed: 27837652]

Gawarammana IB, Buckley NA. Medical management of paraquat ingestion. Br J Clin Pharmacol. 2011; 72:745–57. [PubMed: 21615775]

Gumbiner BM. Signal transduction of beta-catenin. Curr Opin Cell Biol. 1995; 7:634–40. [PubMed: 8573337]

Harris KC, Bielefeld E, Hu BH, Henderson D. Increased resistance to free radical damage induced by low-level sound conditioning. Hear Res. 2006; 213:118–29. [PubMed: 16466871]

Hathaichoti S, Visitnonthachai D, Ngamsiri P, Niyomchan A, Tsogtbayar O, Wisessaowapak C, Watcharasit P, Satayavivad J. Paraquat induces extrinsic pathway of apoptosis in A549 cells by induction of DR5 and repression of anti-apoptotic proteins, DDX3 and GSK3 expression. Toxicol In Vitro. 2017; 42:123–129. [PubMed: 28414160]

He J, Ding D, Yu D, Jiang H, Yin S, Salvi R. Modulation of copper transporters in protection against cisplatin-induced cochlear hair cell damage. Journal of Otology. 2011; 6:53–61.

Higashi K, Imamura M, Fudo S, Uemura T, Saiki R, Hoshino T, Toida T, Kashiwagi K, Igarashi K. Identification of functional amino acid residues involved in polyamine and agmatine transport by human organic cation transporter 2. PLoS One. 2014; 9:e102234. [PubMed: 25019617]

Hong GL, Liu JM, Zhao GJ, Wang L, Liang G, Wu B, Li MF, Qiu QM, Lu ZQ. The reversal of paraquat-induced mitochondria-mediated apoptosis by cycloartenyl ferulate, the important role of Nrf2 pathway. Exp Cell Res. 2013; 319:2845–55. [PubMed: 23954820]

Ikpesu TO. Assessment of occurrence and concentrations of paraquat dichloride in water, sediments and fish from Warri River Basin, Niger Delta, Nigeria. Environ Sci Pollut Res Int. 2015; 22:8517–25. [PubMed: 25548014]

Ingoglia F, Visigalli R, Rotoli BM, Barilli A, Riccardi B, Puccini P, Dall'Asta V. Functional characterization of the organic cation transporters (OCTs) in human airway pulmonary epithelial cells. Biochim Biophys Acta. 2015; 1848:1563–72. [PubMed: 25883089]

Jan TA, Chai R, Sayyid ZN, van Amerongen R, Xia A, Wang T, Sinkkonen ST, Zeng YA, Levin JR, Heller S, Nusse R, Cheng AG. Tympanic border cells are Wnt-responsive and can act as progenitors for postnatal mouse cochlear cells. Development. 2013; 140:1196–206. [PubMed: 23444352]

Jee SH, Kuo HW, Su WP, Chang CH, Sun CC, Wang JD. Photodamage and skin cancer among paraquat workers. Int J Dermatol. 1995; 34:466–9. [PubMed: 7591408]

Kavousi-Gharbi S, Jalli R, Rasekhi-Kazerouni A, Habibagahi Z, Marashi SM. Discernment scheme for paraquat poisoning: A five-year experience in Shiraz, Iran. World J Exp Med. 2017; 7:31–39. [PubMed: 28261553]

Keithley EM, Ryan AF, Woolf NK. Fibronectin-like immunoreactivity of the basilar membrane of young and aged rats. J Comp Neurol. 1993; 327:612–7. [PubMed: 8440784]

Kelley MW. Cell adhesion molecules during inner ear and hair cell development, including notch and its ligands. Curr Top Dev Biol. 2003; 57:321–56. [PubMed: 14674486]

Kuo BR, Baldwin EM, Layman WS, Taketo MM, Zuo J. In Vivo Cochlear Hair Cell Generation and Survival by Coactivation of beta-Catenin and Atoh1. J Neurosci. 2015; 35:10786–98. [PubMed: 26224861]

Kuter K, Smialowska M, Wieronska J, Zieba B, Wardas J, Pietraszek M, Nowak P, Biedka I, Roczniak W, Konieczny J, Wolfarth S, Ossowska K. Toxic influence of subchronic paraquat administration on dopaminergic neurons in rats. Brain Res. 2007; 1155:196–207. [PubMed: 17493592]

Lanzoni I, Corbacella E, Ding D, Previati M, Salvi R. MDL 28170 attenuates gentamicin ototoxicity. Audiological Med. 2005; 3:82–89.

Leonova EV, Raphael Y. Organization of cell junctions and cytoskeleton in the reticular lamina in normal and ototoxically damaged organ of Corti. Hear Res. 1997; 113:14–28. [PubMed: 9387983]

Li HF, Zhao SX, Xing BP, Sun ML. Ulinastatin suppresses endoplasmic reticulum stress and apoptosis in the hippocampus of rats with acute paraquat poisoning. Neural Regen Res. 2015a; 10:467–72. [PubMed: 25878598]

Li J, Wu X, Chen Y, Zeng R, Zhao Y, Chang P, Wang D, Zhao Q, Deng Y, Li Y, Alam HB, Chong W. The Effects of Molecular Hydrogen and Suberoylanilide Hydroxamic Acid on Paraquat-Induced Production of Reactive Oxygen Species and TNF-alpha in Macrophages. Inflammation. 2016; 39:1990–1996. [PubMed: 27624060]

Li P, Ding D, Salvi R, Roth JA. Cobalt-Induced Ototoxicity in Rat Postnatal Cochlear Organotypic Cultures. Neurotox Res. 2015b; 28:209–21. [PubMed: 26153487]

Lin DC, Zhang Y, Pan QJ, Yang H, Shi ZZ, Xie ZH, Wang BS, Hao JJ, Zhang TT, Xu X, Zhan QM, Wang MR. PLK1 Is transcriptionally activated by NF-kappaB during cell detachment and enhances anoikis resistance through inhibiting beta-catenin degradation in esophageal squamous cell carcinoma. Clin Cancer Res. 2011; 17:4285–95. [PubMed: 21610149]

Lindenau J, Noack H, Possel H, Asayama K, Wolf G. Cellular distribution of superoxide dismutases in the rat CNS. Glia. 2000; 29:25–34. [PubMed: 10594920]

Liotta LA, Kohn E. Anoikis: cancer and the homeless cell. Nature. 2004; 430:973–4. [PubMed: 15329701]

Liu B, Qu L, Yang Z, Tao H. Cyclooxygenase-2 inhibitors induce anoikis in osteosarcoma via PI3K/Akt pathway. Med Hypotheses. 2012; 79:98–100. [PubMed: 22546756]

Liu H, Ding D, Sun H, Jiang H, Wu X, Roth JA, Salvi R. Cadmium-induced ototoxicity in rat cochlear organotypic cultures. Neurotox Res. 2014; 26:179–89. [PubMed: 24577639]

Lu J, Tan M, Cai Q. The Warburg effect in tumor progression: mitochondrial oxidative metabolism as an anti-metastasis mechanism. Cancer Lett. 2015; 356:156–64. [PubMed: 24732809]

Mahendrasingam S, Katori Y, Furness DN, Hackney CM. Ultrastructural localization of cadherin in the adult guinea-pig organ of Corti. Hear Res. 1997; 111:85–92. [PubMed: 9307314]

Mizutari K, Fujioka M, Hosoya M, Bramhall N, Okano HJ, Okano H, Edge AS. Notch inhibition induces cochlear hair cell regeneration and recovery of hearing after acoustic trauma. Neuron. 2013; 77:58–69. [PubMed: 23312516]

Mollace V, Iannone M, Muscoli C, Palma E, Granato T, Rispoli V, Nistico R, Rotiroti D, Salvemini D. The role of oxidative stress in paraquat-induced neurotoxicity in rats: protection by non peptidyl superoxide dismutase mimetic. Neuroscience Letters. 2003; 335:163–6. [PubMed: 12531458]

Mosser DM, Edwards JP. Exploring the full spectrum of macrophage activation. Nat Rev Immunol. 2008; 8:958–69. [PubMed: 19029990]

Nicotera TM, Ding D, McFadden SL, Salvemini D, Salvi R. Paraquat-induced hair cell damage and protection with the superoxide dismutase mimetic m40403. Audiol Neurootol. 2004; 9:353–62. [PubMed: 15467288]

Pani G, Giannoni E, Galeotti T, Chiarugi P. Redox-based escape mechanism from death: the cancer lesson. Antioxid Redox Signal. 2009; 11:2791–806. [PubMed: 19686053]

Paoli P, Giannoni E, Chiarugi P. Anoikis molecular pathways and its role in cancer progression. Biochim Biophys Acta. 2013; 1833:3481–98. [PubMed: 23830918]

Park MY, Lee RH, Lee SH, Jung JS. Apoptosis induced by inhibition of contact with extracellular matrix in mouse collecting duct cells. Nephron. 1999; 83:341–51. [PubMed: 10575296]

Prakash Krishnan Muthaiah V, Ding D, Salvi R, Roth JA. Carbaryl-induced ototoxicity in rat postnatal cochlear organotypic cultures. Environ Toxicol. 2017; 32:956–969. [PubMed: 27296064]

Qu X, Zou Z, Sun Q, Luby-Phelps K, Cheng P, Hogan RN, Gilpin C, Levine B. Autophagy gene-dependent clearance of apoptotic cells during embryonic development. Cell. 2007; 128:931–46. [PubMed: 17350577]

Rappold PM, Cui M, Chesser AS, Tibbett J, Grima JC, Duan L, Sen N, Javitch JA, Tieu K. Paraquat neurotoxicity is mediated by the dopamine transporter and organic cation transporter-3. Proc Natl Acad Sci U S A. 2011; 108:20766–71. [PubMed: 22143804]

Reddig PJ, Juliano RL. Clinging to life: cell to matrix adhesion and cell survival. Cancer Metastasis Rev. 2005; 24:425–39. [PubMed: 16258730]

Rybak LP, Ramkumar V. Ototoxicity. Kidney Int. 2007; 72:931–5. [PubMed: 17653135]

Rytomaa M, Martins LM, Downward J. Involvement of FADD and caspase-8 signalling in detachment-induced apoptosis. Curr Biol. 1999; 9:1043–6. [PubMed: 10508619]

Sala-Rabanal M, Li DC, Dake GR, Kurata HT, Inyushin M, Skatchkov SN, Nichols CG. Polyamine transport by the polyspecific organic cation transporters OCT1, OCT2, and OCT3. Mol Pharm. 2013; 10:1450–8. [PubMed: 23458604]

Salvi R, Ding DL, McFadden SL, Salvemini D. M40403, a superoxide dismutase mimetic, prevents hair cell loss in gentamicin-treated cochlear cultures. International Symposium: PHARMACOLOGICAL PROTECTION OF THE INNER EAR. 2002

Samson J, Wiktorek-Smagur A, Politanski P, Rajkowska E, Pawlaczyk-Luszczynska M, Dudarewicz A, Sha SH, Schacht J, Sliwinska-Kowalska M. Noise-induced time-dependent changes in oxidative stress in the mouse cochlea and attenuation by D-methionine. Neuroscience. 2008; 152:146–50. [PubMed: 18234425]

Shi F, Hu L, Jacques BE, Mulvaney JF, Dabdoub A, Edge AS. beta-Catenin is required for hair-cell differentiation in the cochlea. J Neurosci. 2014; 34:6470–9. [PubMed: 24806673]

Shopova VL, Dancheva VY, Salovsky PT, Stoyanova AM, Lukanov TH. Protective effect of U-74389G on paraquat induced pneumotoxicity in rats. Environ Toxicol Pharmacol. 2007; 24:167–73. [PubMed: 21783806]

Silva R, Carmo H, Vilas-Boas V, Barbosa DJ, Monteiro M, de Pinho PG, de Lourdes Bastos M, Remiao F. Several transport systems contribute to the intestinal uptake of Paraquat, modulating its cytotoxic effects. Toxicol Lett. 2015; 232:271–83. [PubMed: 25455457]

Simonneau L, Gallego M, Pujol R. Comparative expression patterns of T-, N-, E-cadherins, beta-catenin, and polysialic acid neural cell adhesion molecule in rat cochlea during development: implications for the nature of Kolliker's organ. J Comp Neurol. 2003; 459:113–26. [PubMed: 12640664]

Stupack DG, Puente XS, Boutsaboualoy S, Storgard CM, Cheresh DA. Apoptosis of adherent cells by recruitment of caspase-8 to unligated integrins. J Cell Biol. 2001; 155:459–70. [PubMed: 11684710]

Sun H, Chen J, Qian W, Kang J, Wang J, Jiang L, Qiao L, Chen W, Zhang J. Integrated long non-coding RNA analyses identify novel regulators of epithelial-mesenchymal transition in the mouse model of pulmonary fibrosis. J Cell Mol Med. 2016; 20:1234–46. [PubMed: 26824344]

Taddei ML, Giannoni E, Fiaschi T, Chiarugi P. Anoikis: an emerging hallmark in health and diseases. J Pathol. 2012; 226:380–93. [PubMed: 21953325]

Takatani T, Takahashi K, Uozumi Y, Shikata E, Yamamoto Y, Ito T, Matsuda T, Schaffer SW, Fujio Y, Azuma J. Taurine inhibits apoptosis by preventing formation of the Apaf-1/caspase-9 apoptosome. Am J Physiol Cell Physiol. 2004; 287:C949–53. [PubMed: 15253891]

Takeichi M. Morphogenetic roles of classic cadherins. Curr Opin Cell Biol. 1995; 7:619–27. [PubMed: 8573335]

Tona Y, Hamaguchi K, Ishikawa M, Miyoshi T, Yamamoto N, Yamahara K, Ito J, Nakagawa T. Therapeutic potential of a gamma-secretase inhibitor for hearing restoration in a guinea pig model with noise-induced hearing loss. BMC Neurosci. 2014; 15:66. [PubMed: 24884926]

Valentijn AJ, Zouq N, Gilmore AP. Anoikis. Biochem Soc Trans. 2004; 32:421–5. [PubMed: 15157151]

Wang J, Ding D, Shulman A, Stracher A, Salvi RJ. Leupeptin protects sensory hair cells from acoustic trauma. Neuroreport. 1999; 10:811–6. [PubMed: 10208553]

Wang Q, Liu S, Hu D, Wang Z, Wang L, Wu T, Wu Z, Mohan C, Peng A. Identification of apoptosis and macrophage migration events in paraquat-induced oxidative stress using a zebrafish model. Life Sci. 2016; 157:116–24. [PubMed: 27288846]

Warchol ME. Cell density and N-cadherin interactions regulate cell proliferation in the sensory epithelia of the inner ear. J Neurosci. 2002; 22:2607–16. [PubMed: 11923426]

Warchol ME. Characterization of supporting cell phenotype in the avian inner ear: implications for sensory regeneration. Hear Res. 2007; 227:11–8. [PubMed: 17081713]

Wesseling C, van Wendel de Joode B, Ruepert C, Leon C, Monge P, Hermosillo H, Partanen TJ. Paraquat in developing countries. Int J Occup Environ Health. 2001; 7:275–86. [PubMed: 11783857]

Whitlon DS. E-cadherin in the mature and developing organ of Corti of the mouse. J Neurocytol. 1993; 22:1030–8. [PubMed: 8106878]

Yamada A, Aki T, Unuma K, Funakoshi T, Uemura K. Paraquat induces epithelial-mesenchymal transition-like cellular response resulting in fibrogenesis and the prevention of apoptosis in human pulmonary epithelial cells. PLoS One. 2015; 10:e0120192. [PubMed: 25799450]

Yang W, Vethanayagam RR, Dong Y, Cai Q, Hu BH. Activation of the antigen presentation function of mononuclear phagocyte populations associated with the basilar membrane of the cochlea after acoustic overstimulation. Neuroscience. 2015; 303:1–15. [PubMed: 26102003]

Yon JM, Baek IJ, Lee SR, Jin Y, Kim MR, Nahm SS, Kim JS, Ahn B, Lee BJ, Yun YW, Nam SY. The spatio-temporal expression pattern of cytoplasmic Cu/Zn superoxide dismutase (SOD1) mRNA during mouse embryogenesis. J Mol Histol. 2008; 39:95–103. [PubMed: 17786570]

Yu J, Ding D, Sun H, Salvi R, Roth JA. Neurotoxicity of trimethyltin in rat cochlear organotypic cultures. Neurotox Res. 2015; 28:43–54. [PubMed: 25957118]

Zhang M, Liu W, Ding D, Salvi R. Pifithrin-alpha suppresses p53 and protects cochlear and vestibular hair cells from cisplatin-induced apoptosis. Neurosci. 2003; 120:191–205.

Zheng JL, Gao WQ. Overexpression of Math1 induces robust production of extra hair cells in postnatal rat inner ears. Nat Neurosci. 2000; 3:580–6. [PubMed: 10816314]

Highlights

- Paraquat generates superoxide radical that damages cochlear explants
- Paraquat damage progresses from tympanic border cells, to Deiters cells and finally hair cells
- Cell death in the Deiters cell layer is associated with increased caspase-8 expression
- Paraquat decreases E-cadherin and b-catenin expression in supporting cells prior to hair cell death
- Supporting cell loss may contribute to anoikis-like apoptosis in hair cells

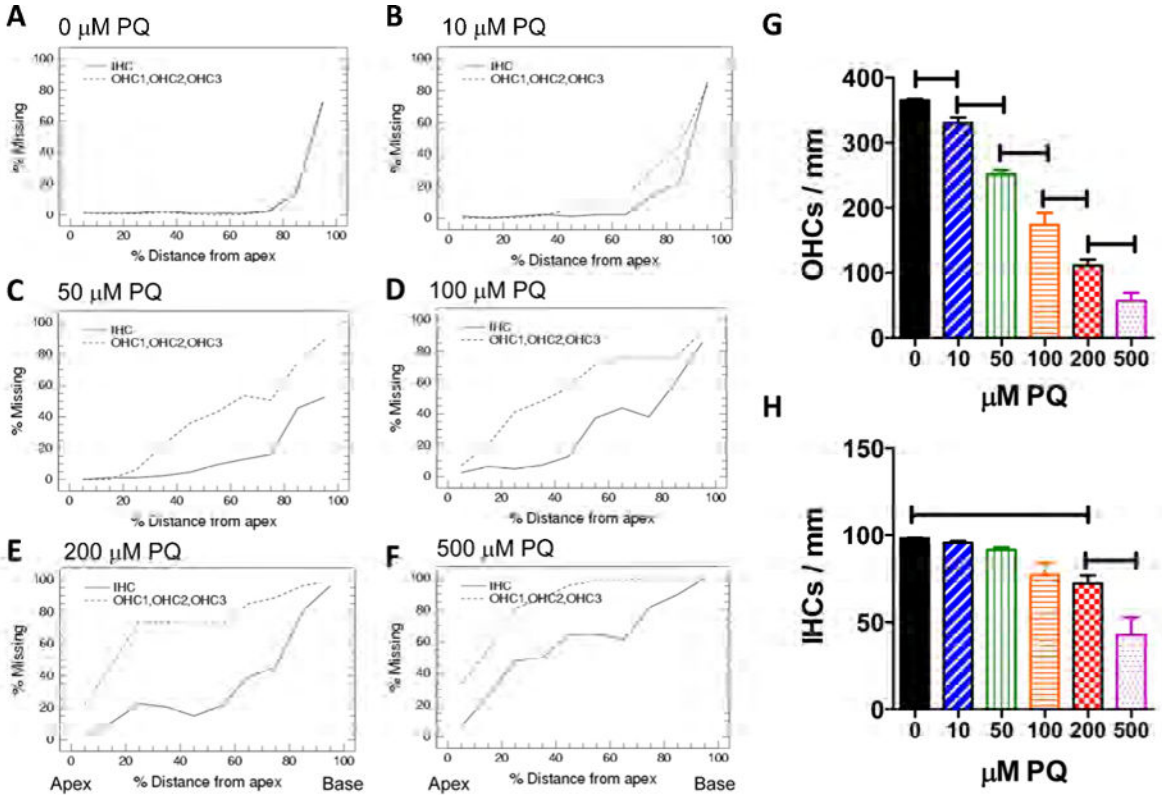

Figure 1.

(A–F) Mean (n=6 cochlea per group) cochleograms showing the percent missing OHCs (dashed line) and IHCs (solid line) as a function of percent distance from the apex of the cochlea. Cochlear organotypic cultures treated for 24 h with increasing concentrations of PQ ranging from 0 to 500 μM as indicated above each panel. (G) Mean (+SEM, n=6 cochlea per group) OHC density (3 rows OHC/mm) and (H) mean (+SEM, n=6 cochlea per group) IHC density (IHC/mm) as a function of PQ dose (0 to 500 μM). Lines show PQ treatments in which the mean hair cell densities were significantly ($p < 0.05$) different from the next lowest dose of PQ.

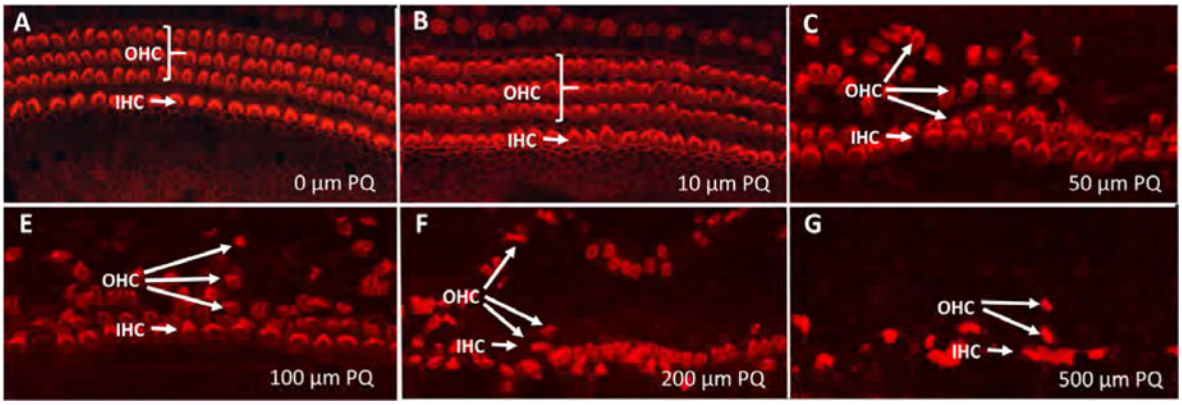

Figure 2.

Representative surface preparations from cochlear explants treated for 24 h with PQ doses from 0–500 µM as indicates in panels A–G. (A) Control culture illustrating stereocilia and cuticular plate of three rows of outer hair cells (OHC) and one row of inner hair cells (IHC) labeled with Alexa Fluor 555-conjugated phalloidin that labels F-actin expressed in stereocilia and hair cell cuticular plate. Note orderly rows of OHCs and IHCs in panels A–B and disorderly rows of hair cells and dislocated OHC rows in panels C–G.

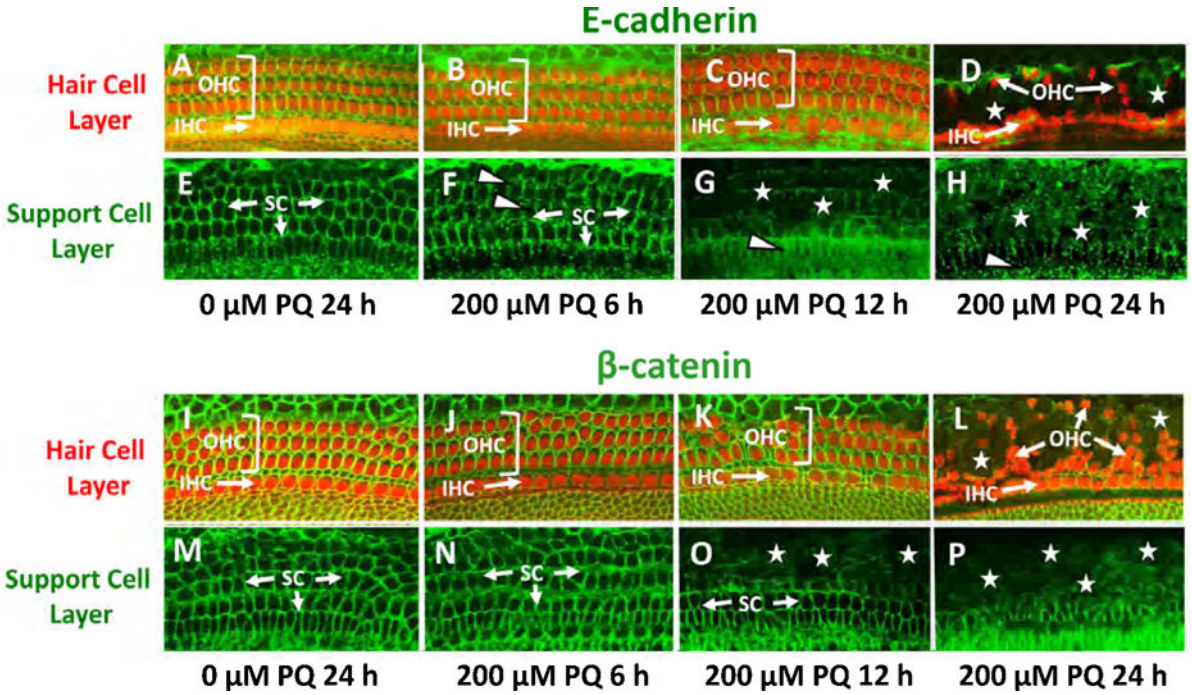

Figure 3.

Representative radial sections (3 µm) of cochlear organotypic cultures stained with toluidine blue. (A) Control (0 µM) sample cultured for 24 h showing three rows of outer hair cells (OHC), one row of inner hair cells (IHC), Deiters cells (DC, green arrow), inner and outer pillar cells (PC, pink arrow), inner sulcus cells (ISC, white arrow), basilar membrane (dashed line) and tympanic border cells (TBC) beneath the basilar membrane. (B) Section from culture treated for 6 h with 200 µM PQ. OHC and IHC still present, missing or severely shrunken TBC indicated by arrowhead beneath the basilar membrane. Note pale cytoplasm in remaining TBC and shrunken DC with pale cytoplasm. (C) Section from culture treated for 12 h with 200 µM PQ. IHC and OHC still present; missing DC labeled with *; many missing or severely shrunken TBC (arrowhead). (D) Section from culture treated with 200 µM PQ for 24 h. Remaining IHC and OHC are pale and shrunken. Note missing DC (*) and TBC (arrowhead).

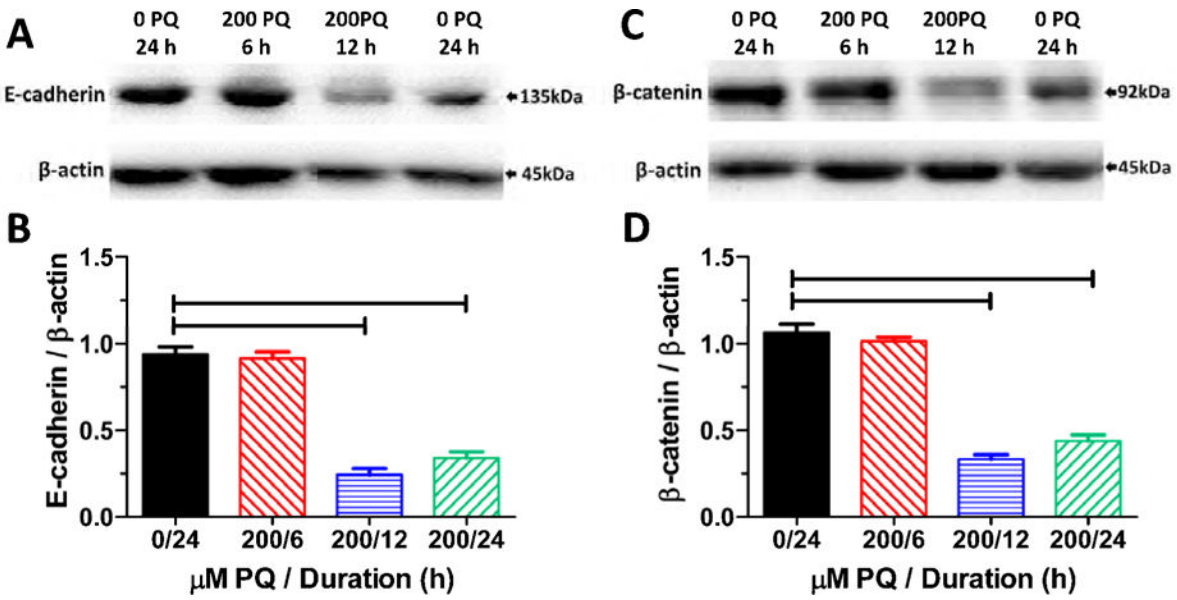

Figure 4.

Early support cell destruction. Z-plane section and surface view of cochlear explants cultured for 24 h without PQ (A1, A2, 0 μM) or cultured with 200 μM PQ for 6 h (B1, B2), 12 h (C1, C2) or 24 h (D1, D2). Specimens stained with To-Pro-3 (blue), which labels nuclei, a SOX2 antibody (green) that labels support cells and a myosin VI antibody (red) that labels the cytoplasm of outer hair cells (OHC) and inner hair cells (IHC). Hensen cells (HC), Deiters cells (DC), pillar cells (PC) and inner sulcus cells (ISC) show strong SOX2/ ToPro-3 (turquoise=green/blue merge) labeling. (A1) In normal explants, HC are lateral to OHC, DCs are below OHC and PC are below first OHC row and IHC. (A2) Surface image stack shows orderly rows of OHC and underlying DC (turquoise with red fringe) and IHC (red cytoplasm, blue nucleus). (B1, B2) After 6 h treatment with 200 μM PQ, many HC and a few DC are missing. Most OHC and IHC are present. (C1, C2) After 12 h treatment with 200 μM PQ, most DC and few OHC and IHC are missing. (D1, D2) After 24 h treatment with 200 μM PQ, most support cells and OHC are missing near the lateral edge of the epithelium. Some IHC and PC are present in an irregular row bordering the ISC region.

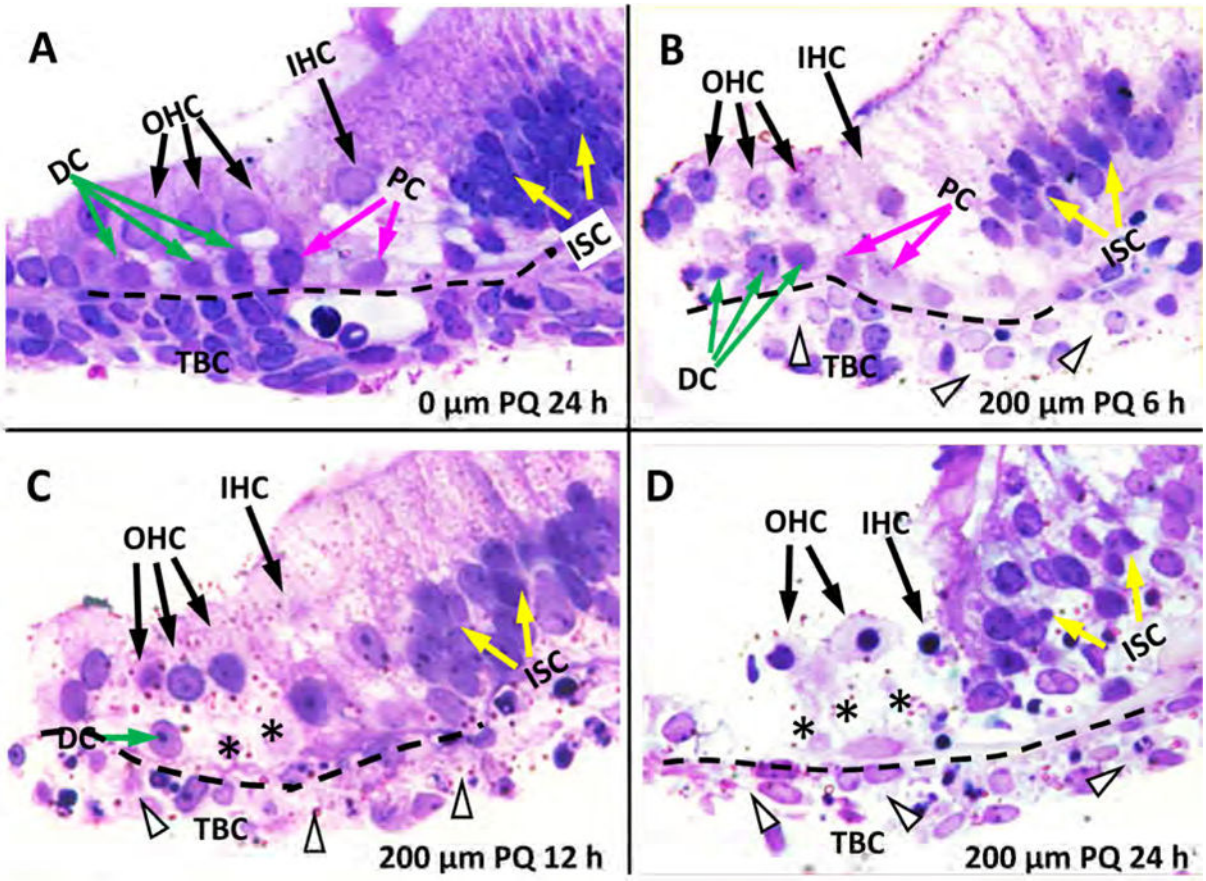

Figure 5.

Detection of superoxide by DHE fluorescent labeling. Specimens labeled with To-Pro-3 to label nuclei (blue), DHE (red) or Alexa 488-conguated phalloidin (green) to label the stereocilia and cuticular plate of hair cells. (A) Z-plane section from untreated cochlear explant cultured for 24 h shows negligible DHE fluorescent labeling in support cell layer (SC, bracket) and outer hair cells (OHCs) and inner hair cells (IHCs). (B) Treatment for 6 h with 200 µM induces DHE fluorescence (fuchsia color represents overlap of red DHE and blue To-Pro-3, white arrowhead) mainly in SC layer beneath the hair cells including cells beneath the basilar membrane. (C) Treatment for 12 h with 200 µM PQ induces strong DHE fluorescence in SC layer (bracket) including cells beneath the OHC and IHC and cells beneath the basilar membrane. (D) Treatment for 24 h with 200 µM PQ induces DHE fluorescence in OHC region, but little DHE fluorescence in the SC layer; destruction of support cells in deeper layers of the epithelium eliminates fluorescence from this region. (E) Mean gray level measures of superoxide in cochlear explants in untreated group cultured for 24 h, 200 µM PQ treatment for 6 h, 12 h, and 24 h groups. Horizontal lines identify between hair cells and supporting cells differences that were statistically significant (Newman-Keuls, $p<0.05$).

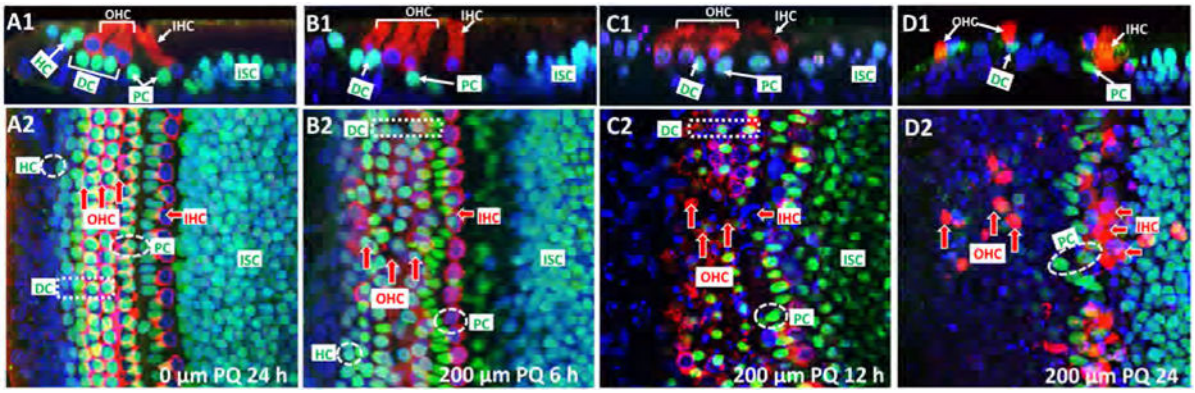

Figure 6.

Caspase expression appears in Deiters cells before hair cell layer. Confocal images from the OHC layer and DC layers of cochlear explants. Alexa-488 conjugated phalloidin (green) used detect actin present in stereocilia and cuticular plate; To-Pro-3 (blue) used to label nuclei and flurogenic probe to detect activated (A1–4) caspase-8, (B1–4) caspase-9 and (C1–4) caspase-3 (C1–4) (red). Representative samples from the middle of the cochlea from control explant 24 h (0 µM PQ, top row) and explants treated with 200 µM PQ for 6 h (second row from top), 12 h (third row from top) and 24 h (bottom row). Caspase-8 (A2b) and to a lesser extent caspase-3 (C2b) first expressed in DC layer after 6 h of PQ treatment; caspase-8, -9 and -3 expression in OHC layer occurred after 24 h of PQ treatment (A4a, B4a, C4a), but many OHC already missing at this time (see Figure 3E). Caspase-9 expression first observed in DC layer (B3b). Mean (n=5, +/− SD) numbers of caspase-8 (D), caspase-9 (E) and caspase-3 (F) cells present in OHC layer and DC layer in control explants (0 µM PQ, 24 h) and explants treated with 200 µM PQ for 6, 12 or 24 h. Note robust increase in caspase-8 and caspase-3 in DC layer after 6 h PQ treatment. Increase in caspase-8, -9 and -3 expression in OHC layer occurred after 24 PQ, but many OHC were already missing at this time (Figure 3E).

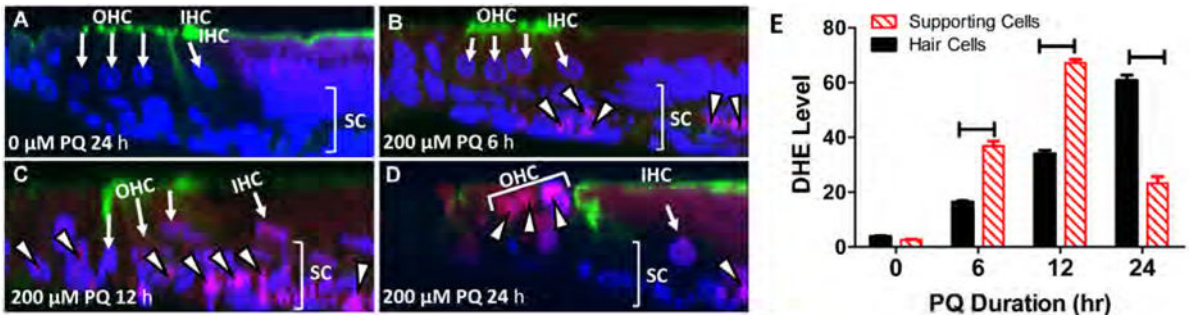

Figure 7.

PQ suppresses E-cadherin and β-catenin immunolabeling. (A–E) Cochlear explants immunolabeled with antibody against E-cadherin (green) and Alexa Fluor 555-conjugated phalloidin (red) which labels F-actin that is heavily expressed in the hair cell cuticular plate. Confocal images taken from the upper hair cell layer (top row) and lower supporting cell layer (2nd row from top) of a control explant cultured for 24 h (A, E) and explants treated with 200 mM PQ for 6 h (B, F), 12 h (C, G) and 24 h (D, H). (A) In upper hair cell layer of a control explant, phalloidin labled outer hair cells (OHC) and inner hair cells (IHC) (red/orange) are surrounded by E-cadherin (green). (D) After 24 h PQ treatment, most IHCs were present, many OHC were missing and most E-cadherin labeling had disappeared. (E) In the support cell layer, rings of E-cadherin were present in the SCs (arrows) in the control culture, but in the culture treated with PQ for 6 h (SC, green) the ring of E-cadherin was discontinuos and crenulated in some regions (arrowheads). (G–H) After 6 h and 12 h PQ treatment, much of the E-cadherin had disappeared. (I–P) Cochlear explants immunolabeled with antibodies against β-catenin (green) and Alexa Fluor 555-conjugated phalloidin (red) which labels F-actin that is heavily expressed in the hair cell cuticular plate. Confocal images taken from the upper hair cell layer (2nd row from bottom) and lower supporting cell layer (bottom row) of a control explant (I, M) cultured for 24 h and explants treated with 200 mM PQ for 6 h (J, N), 12 h (K, O) and 24 h (L, P). (I) In upper hair cell layer of control, the phalloidin-labled outer hair cells (OHC) and inner hair cells (IHC) (red/orange) were surrounded by β-catenin (green). (L) After 24 h PQ treatment, most IHCs were present, but many OHC were missing and most β-catenin had disappeared. (M–P) In the support cell layer, rings of β-cadherin were present in the SCs in the control culture and PQ culture treated for 6 h (SC, arrow, green). (O) After 12 h PQ treatment, the rings of β-cadherin had started to disappear in the OHC region and (P) after 24 h PQ treatment, much of the β-cadherin was missing except near the IHC region.

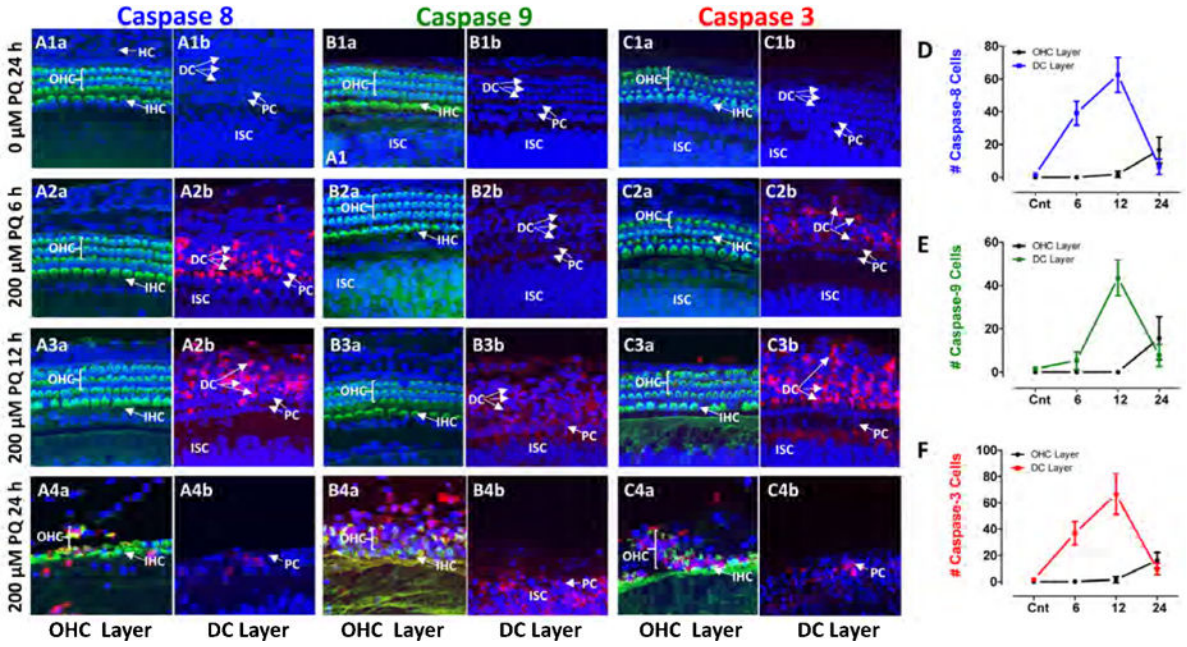

Figure 8.

(A) Western blots of E-cadherin and β-actin obtained from control explant cultured for 24 h (0 PQ, 24 h) and explants treated with 200 µM PQ and cultured for 6, 12 or 24 h. (B) Mean (SEM, n=3 replicates/condition, 6 or more cochlear/measurement) values of E-cadherin relative to β-actin in controls explants (0 PQ, 24 h) and explants treated with 200 µM PQ for 6, 12 or 24 h. (C) Western blots of β-catenin and β-actin obtained from control explants cultured for 24 h (0 PQ, 24 h) and explants treated with 200 µM PQ and cultured for 6, 12 or 24 h. (D) Mean (SEM, n=3 replicates/condition; 6 or more cochlea/measurement) values of β-catenin relative to β-actin in controls explants (0 PQ, 24 h) and explants treated with 200 µM PQ for 6, 12 or 24 h. Horizontal bars identify PQ treatment durations that were significantly different from controls ($p<0.05$).